Chapter 4

A Surface-Coupled Optical Trap with 1-bp Precision via Active Stabilization

Stephen R. Okoniewski, Ashley R. Carter, and Thomas T. Perkins

Abstract

Optical traps can measure bead motions with Å-scale precision. However, using this level of precision to infer 1-bp motion of molecular motors along DNA is difficult, since a variety of noise sources degrade instrumental stability. In this chapter, we detail how to improve instrumental stability by (1) minimizing laser pointing, mode, polarization, and intensity noise using an acousto-optical-modulator mediated feedback loop and (2) minimizing sample motion relative to the optical trap using a three-axis piezo-electric-stage mediated feedback loop. These active techniques play a critical role in achieving a surface stability of 1 Å in 3D over tens of seconds and a 1-bp stability and precision in a surface-coupled optical trap over a broad bandwidth ($\Delta f = 0.03$ –2 Hz) at low force (6 pN). These active stabilization techniques can also aid other biophysical assays that would benefit from improved laser stability and/or Å-scale sample stability, such as atomic force microscopy and super-resolution imaging.

Key words Optical trap, Optical tweezers, Single molecule, Active stabilization, Force spectroscopy

1 Introduction

Optical traps can apply controlled forces to individual biomolecular complexes and measure motions of molecular motors along their substrates with exquisite precision. As a result, advances in the precision and stability of optical traps have yielded many landmark results in single-molecule biophysics, including resolving the steps of kinesin [1], myosin [2], RNA polymerase [3], and the ribosome [4]. A number of excellent articles review the construction and application of optical traps [5–9].

While optical traps can resolve Å-scale bead displacements in a millisecond [5, 10, 11], reaching a similar level of precision and stability in a biophysical assay is much more challenging. Consider the surface-coupled optical trap depicted in Fig. 1a. A DNA molecule is stretched between a surface and an optically trapped bead. Unwanted motion in the surface or trap position degrades the positional precision of the single-molecule assay. However, by

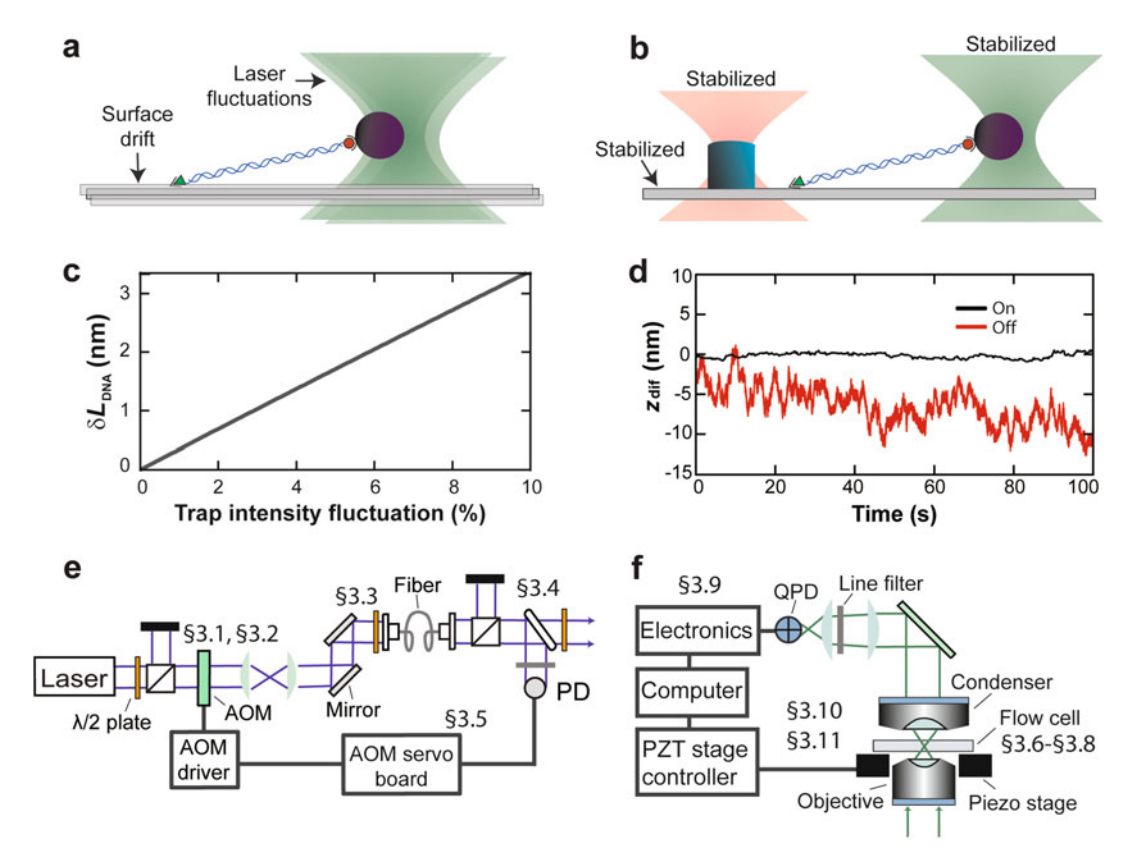


Fig. 1 (a) Schematic of a surface-coupled optical-trapping assay used to measure motion of an enzyme along DNA. A DNA molecule is anchored to a glass coverslip at one end and to an optically trapped bead at the other. Surface drift and laser pointing fluctuations corrupt measurements of DNA length. (b) An actively stabilized surface-coupled optical-trapping assay where the sample surface is stabilized by keeping the position of a fiducial mark fixed relative to a detection laser. Each laser is stabilized with an acousto-optic modulator (AOM)-mediated feedback loop. Not shown: a third laser that is collinear with the trapping laser for independent bead detection. The assay precision arises from excellent differential-pointing stability between the three lasers' foci. (c) Intensity noise affects trapped bead position under load and thereby measurements of DNA contour length (L_{DNA}). For a typical DNA length in a surface-coupled assay ($L_{DNA} = 1,000$ nm) under 6 pN of load, variations in contour length (δL_{DNA}) increase linearly with fluctuations in the trapping laser intensity. Intensity fluctuations of a few percent result in nm-scale apparent variations in L that can mask bpsized motions (reprinted with permission from ref. [13]; © 2009 Elsevier). (d) The difference in the vertical position of a common object (z_{diff}) measured by two detection lasers plotted as a function of time. In threedimensional back-focal-plane detection [10], the vertical position signal is proportional to the total light on the detector. Hence, a measurement of zdiff using unstabilized lasers shows significantly more noise than a measurement where both lasers are stabilized and their sum signals are offset amplified (see Subheading 3.9). (Reprinted with permission from ref. [12]; © 2007 The Optical Society). (e) Optics diagram of the trapping laser with its stabilization feedback loop (PD: photodiode; λ/2; half-wave plate). Construction and tuning of this feedback loop is covered in Subheadings 3.1-3.5. (f) Schematic of a surface-stabilization feedback loop where the optical signal is electronically processed and a computer-based feedback loop moves the sample surface via a piezo-electric (PZT) stage. Construction and implementation of this feedback loop is covered in Subheadings 3.6–3.11 (QPD: quadrant photodiode)

actively stabilizing the sample surface [12] and the trapping laser (Fig. 1b) [13], one can more precisely measure the extension and tension of the DNA [14]. Ideally, this measurement is limited by the Brownian motion of the bead. Since such thermal motion has a zero mean, spatial precision is often increased at the cost of temporal resolution by time-averaging the bead motion. This strategy does not yield increased precision if instrumental noise sources—like drift in the sample surface or pointing noise in the laser—dominate the measured motion. These noise sources corrupt the measurement process. For example, variations in the stiffness of the optical trap due to laser-intensity fluctuations cause apparent changes in the DNA length (Fig. 1c). Intensity fluctuations also degrade the precision with which one can measure the vertical position of the bead, or, more relevant to this chapter, the vertical position of a fiducial mark on the sample surface with a detector beam (Fig. 1d). To obtain 1-bp (base pair) precision along DNA, the adverse effects of instrumental noise on bead-position measurements must be reduced to $\leq 1 \text{ Å } [3, 9]$.

These instrumental noise sources are typically reduced through a combination of passive and active stabilization techniques. Passive techniques tend to reduce noise by isolating the experiment from the noise source. For example, a floating optical table isolates the experiment from environmental vibrations, and an enclosure around the optics minimizes beam-pointing fluctuations by reducing air currents. An excellent example of passive stabilization is the dual-beam optical trap, which decouples the single-molecule assay from the surface and thereby isolates it from surface noise [15]. Active techniques use feedback; they measure the amount of noise in the system, and modulate some parameter(s) of the system in real time to reduce that noise.

In this chapter, we detail how to apply active-stabilization techniques to minimize laser noise in a surface-coupled opticaltrapping instrument and to stabilize the surface relative to the optical-trapping laser (Fig. 1b) as a means to achieve 1-bp precision and stability in single-molecule assays. To minimize a variety of sources of laser noise, we first pass the laser through an acoustooptic modulator (AOM) and a single-mode, polarizationmaintaining optical fiber. Coupling the laser into the fiber transforms pointing and mode noise into intensity noise. We then measure the intensity after the laser exits the fiber and use that signal to stabilize the laser intensity via the AOM (Fig. 1e). To minimize surface motion, we attach fiducial marks to the coverslip so that unwanted sample motion can be measured using a lowerpowered "detector" laser. The coverslip is then mounted on a three-axis piezo-electric (PZT) stage, which can move with Å-scale precision to compensate for the unwanted surface motion (Fig. 1f). This combination of active laser and surface stabilization enables our instrument to achieve 1-bp stability ($\Delta f = 0.03-2$ Hz)

at a relatively low load (6 pN), with higher precision and larger bandwidth achieved at higher forces.

In the first five sections of this chapter, we detail how to create the laser stabilization feedback loop (Fig. 2). Subheading 3.1 explains the installation of an AOM system, and Subheading 3.2 details the AOM-laser alignment needed to achieve the best performance. Subheading 3.3 discusses coupling the resulting first-order AOM-diffracted laser beam into a single-mode, polarization-maintaining optical fiber. Subheading 3.4 details sampling 10 % of the laser intensity after a subsequent fiber launch onto a photodiode for intensity stabilization, and Subheading 3.5 provides the details on building and testing an AOM servo-circuit board; these electronics transform the photodiode's intensity signal into a control signal for the AOM.

The last six sections of this chapter detail how to create the surface-stabilization feedback loop. Subheadings 3.6, 3.7, and 3.8 detail creating a sample chamber with an array of fiducial marks fabricated onto the interior of a coverslip. Subheading 3.9 provides the schematic for building an offset-amplifier, so that the vertical position of a fiducial mark can be more precisely detected and thereby stabilized. Subheading 3.10 explains vertically aligning multiple lasers to maximize sensitivity and aligning a detector laser to a fiducial mark (*see* **Note 1**). Finally, Subheading 3.11 discusses the software design and implementation of the surface-stabilization feedback loop and testing the performance of the stabilization using an out-of-loop monitor.

2 Materials

2.1 Installing an AOM System

- 1. Near-infrared (NIR) laser (for either trapping or detection).
- 2. Single-beam NIR AOM (Isomet, model 1205C-2, PbMoO₄ crystal. Anti-reflection coated).
- 3. Fixed-frequency analog-modulation driver (Isomet, our model: 232A-2, new model: 532C-2).
- 4. Four-axis tilt aligner (Newport, model 9071, 3 mm & 8° travel).
- 5. Machined mount for tilt aligner.
- 6. +28 V 1 A DC (direct current) power supply (Isomet).
- 7. Electrical soldering iron.
- 8. Heat sink for modulation driver.
- 9. Thermal paste.
- 10. BNC cables and SMA-to-BNC, SMB-to-BNC converters (Isomet).
- 11. Controllable DC-voltage source.
- 12. Optics table.

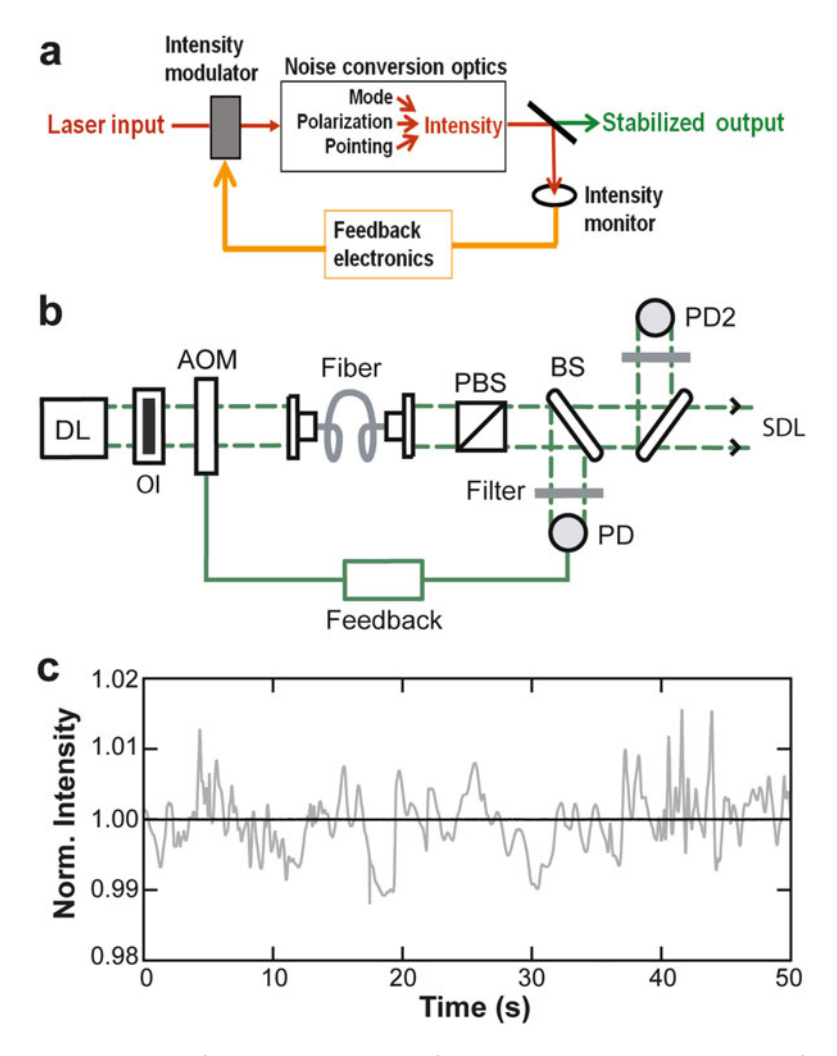


Fig. 2 (a) Conceptual diagram of the laser stabilization feedback loop where several types of laser noise are converted into intensity noise. The intensity noise is measured and then minimized using a feedback loop. The advantage of this scheme is the exact magnitude of different types of laser noise does not need to be known. (b) Optics diagram for implementing the laser stabilization feedback loop shown in (a). A second photodiode (PD) is shown and is used to characterize the performance of the feedback loop using an out-of-loop monitor (*DL* diode laser, *Ol* optical isolator, *BS* beam splitter). (c) A plot of normalized laser intensity versus time, prior to stabilization (*gray*) and after stabilization (*black*) for a 785-nm detection laser. Data were averaged to 100 Hz (reprinted with permission from ref. [12]; © 2007 The Optical Society)

2.2 Maximizing the Diffraction Efficiency of a Laser through an AOM

- 1. The AOM system from Subheading 3.1.
- 2. Two plano-convex lenses (Thorlabs, N-BK7 material, focal lengths determined by available space).
- 3. Fiber bench (Thorlabs, model FB-38).

- 4. Half-wave plate, fiber bench mountable (Thorlabs, model RABH-980).
- 5. PBS cube, fiber bench mountable (Newport, model 05FC16PB.5).
- 6. Beam block (Thorlabs, model LB1).
- 7. Power meter (Thorlabs, model PM100D with S130C detector).
- 8. NIR detection card.
- 9. Laser safety glasses.

2.3 Coupling the First-Order AOM Diffraction into an Optical Fiber

- 1. The optical system from Subheading 3.2.
- 2. Beam block or iris.
- 3. Two plano-convex lenses (Thorlabs, N-BK7 material, focal lengths determined by available space).
- 4. Two NIR mirrors (Thorlabs, model BB1-E03).
- 5. Fiber bench with wall plates and dust cover (Thorlabs, model FB-38W).
- 6. Half-wave plate, fiber bench mountable (Thorlabs, model RABH-980).
- 7. Fiber coupler (Thorlabs, FiberPort model PAF-X-5-B).
- 8. Polarization-maintaining fiber-optic patch cable, panda style, one FC/APC and one FC/PC connector (OZ Optics).
- 9. Machined clamp for patch cable stabilization.
- 10. Laser pointer for fiber-optic testing (FC male head).

2.4 Launching the Laser and Monitoring the Fiber Output Intensity with a Photodiode

- 1. Fiber-optic patch cable from Subheading 3.3.
- 2. Machined clamp for patch cable stabilization.
- 3. Fiber-launch system, free space (Thorlabs, model KT110).
- 4. Mounted aspheric lens (Newport, model 5723-H-B; f = 8 mm, anti-reflection coated).
- 5. Asphere adapter (Newport, model 5709).
- 6. Beam profiler (or razor blade and power meter).
- 7. Plano-convex lens (focal length calculated during aspheric lens installation).
- 8. PBS cube (Newport, model 10FC16PB.5).
- 9. 90/10 beam sampler (Newport, model 10B20NC.2).
- 10. Neutral density filter (Thorlabs, e.g., model ND20A).
- 11. Analog PIN photodiode (Excelitas, model YAG-444AH).
- 12. Power supply for photodiode.
- 13. NIR laser-line filter (e.g., Thorlabs, model FL1064-10).

- 14. Machined mount for photodiode and line filter.
- 15. XY translator (Thorlabs, model ST1XY-D).
- 16. 10-kΩ gain trans-impedance amplifier, *see* circuit diagram at https://jila.colorado.edu/perkins/research/resources.
- 17. Machined housing for photodiode mount and amplifier.
- 2.5 Completing the Feedback Loop with an AOM Servo Board and Checking Performance
- 1. The completed setup from Subheading 3.4.
- 2. See AOM Servo Parts List at https://jila.colorado.edu/perkins/research/resources.
- 3. Spectrum analyzer (SRS, model SRSR780) or oscilloscope (>80 MHz bandwidth).
- 2.6 Cleaning Glass Coverslips
- 1. Magnetic stir plate with large stir bar.
- 2. Ultrasonic bath (Branson 5200).
- 3. 18-M Ω purified water (e.g., from a Thermo Scientific Barnstead Nanopure).
- 4. Microwave.
- 5. Four 1-L beakers.
- 6. One purified water squirt bottle and one ethanol squirt bottle.
- 7. 250 mL completely denatured ethanol (Macron, product number 7018-16).
- 8. 300 mL acetone (Fisher).
- 9. 80 g KOH pellets (Fisher, 0.4 % potassium carbonate).
- 10. Glass coverslips $(22\times40 \text{ mm}, \text{thickness } 1 \text{ } 1/2).$
- 11. Custom-machined Teflon coverslip rack with handle.
- 12. Container for coverslip rack (such as an empty pipette tip box).
- 13. Parafilm.
- 14. Diamond scribe.
- 2.7 Fabricating Fiducial Marks onto Coverslips
- 1. Cleaned coverslips from Subheading 3.6.
- 2. Teflon coverslip rack.
- 3. Container for coverslip rack (such as an empty pipette tip box).
- 4. Gloves.
- 5. Tweezers.
- 6. Hot plate.
- 7. FOx 16 Flowable Oxide (Dow Corning).
- 8. Spin coater.
- 9. Scanning electron microscope (FEI, Nova NanoSEM 630).
- 10. Fume hood.
- 11. Two 50-mL beakers.

- 12. Filtered water.
- 13. TMAH solution (Dow Electronic Materials, MicroPosit MF CD-26, 2.4 % tetramethylammonium hydroxide).
- 14. Nitrogen gas spray gun.
- 15. O₂ plasma etcher (PlasmaSTAR, AXIC).

2.8 Assembling Flow Cells with Fabricated Coverslips

- 1. Fabricated coverslips from Subheading 3.7.
- 2. Microscope slides (Corning, $75 \times 25 \times 1 \text{ mm}^3$).
- 3. Double-sided tape (Scotch, ½ inch wide).
- 4. Scissors.
- 5. Razor blade.
- 6. 5-min epoxy (Devcon).
- 7. Disposable dish (e.g., a weigh boat).
- 8. Pipette tip.
- 9. Custom-machined Teflon mount.

2.9 Processing a QPD Voltage Signal with an Offset Amplifier Circuit Board

- 1. See Offset Amplifier Parts List at https://jila.colorado.edu/perkins/research/resources.
- 2. LabVIEW software.
- 3. PCI board to send computer-controlled voltages (National Instruments, NI-PCI-6703).
- 4. PXI Data Acquisition System (National Instruments) (see Note 2).
 - (i) NI PXIe-1082 PXIe chassis/controller.
 - (ii) NI PXIe-PCIe8375 computer to chassis boards (compatible with Dell and HP PCs).
 - (iii) NI PXIe-6368 Simultaneous X-series data acquisition board.
- 5. Three shielded cables (National Instruments, two SHC68-68-EPM and one SH68-68-D1).
- 6. Three connector blocks (National Instruments, model SCB-68).

2.10 Preparing the Instrument for Surface Stabilization

- 1. The flow cell from Subheading 3.8.
- 2. The setup from Subheading 3.9.
- 3. Three-axis, closed-loop PZT stage (Physik Instrumente, model P-517.3CD).
- 4. PZT stage controller (Physik Instrumente, model E-710. P3D).
- 5. GPIB to USB cable (National Instruments, NI GPIB-USB-B).
- 6. Monolithic slide holder (to be screwed into the piezo stage).
- 7. Mounting accessories for PZT stage (dependent on individual setup).

3 Methods

3.1 Installing an AOM System

To actively stabilize a near-infrared (NIR) laser, we convert its pointing, mode, and polarization noise into intensity noise and then mitigate intensity noise using an AOM-mediated feedback loop (Fig. 2). To create this feedback loop, we first need to install a single-beam NIR AOM system (Fig. 3a). This system is composed of three devices: the AOM, a modulation driver for the AOM (Fig. 3b), and a power supply. The AOM has an SMA input, and two apertures for laser input and output. When an oscillating voltage is applied to the SMA input, a piezoelectric transducer inside of the AOM rapidly expands and contracts in response. These vibrations create a traveling sound wave that varies the refractive index in an attached crystal. If a beam of light passes through the crystal, these index variations act as a diffraction grating (Fig. 3c), diffracting some of the light intensity (Fig. 3d). The amount of diffracted intensity will depend on the amplitude of the sound wave. This amplitude is controlled by a voltage applied to the input of the modulation driver. The angle between the zeroth and first order beams is set by the frequency of the sound wave (see Note 3).

Our modulation driver has three connection points: a power supply input labeled "+Vdc", a voltage input labeled "MOD", and a voltage output labeled "RF", for radio frequency. It also has a control screw labeled "PWR ADJ", and an optional control screw labeled "BIAS ADJ". The output RF signal's amplitude is set by the "MOD" input voltage. The "MOD" and "RF" connectors can be BNC, SMA, or SMB, depending on the driver model; the driver manufacturer should be contacted for purchasing the best cables or converters. To keep the diffracted beam's position fixed in space, we use a fixed-frequency (80 MHz) modulation driver. To power the modulator, we connect the "+Vdc" terminal to a 28 V DC (direct current) power supply regulated to ± 1 % (see Note 4). In addition, the driver must be connected to an external heatsink, which can either be machined or bought. A driver's heatsink requirements are given in its manual.

1. Choose the height you wish to set the optical axis at above the optics table. This is the height at which the laser will propagate. The laser propagation height will determine the height of many of the optics in this system. This height is largely a matter of convenience, but shorter is generally better, as it will make the optics less susceptible to mechanical vibrations. Denote this height as y_0 , in a coordinate system with z pointing along the optical axis (see Note 5).

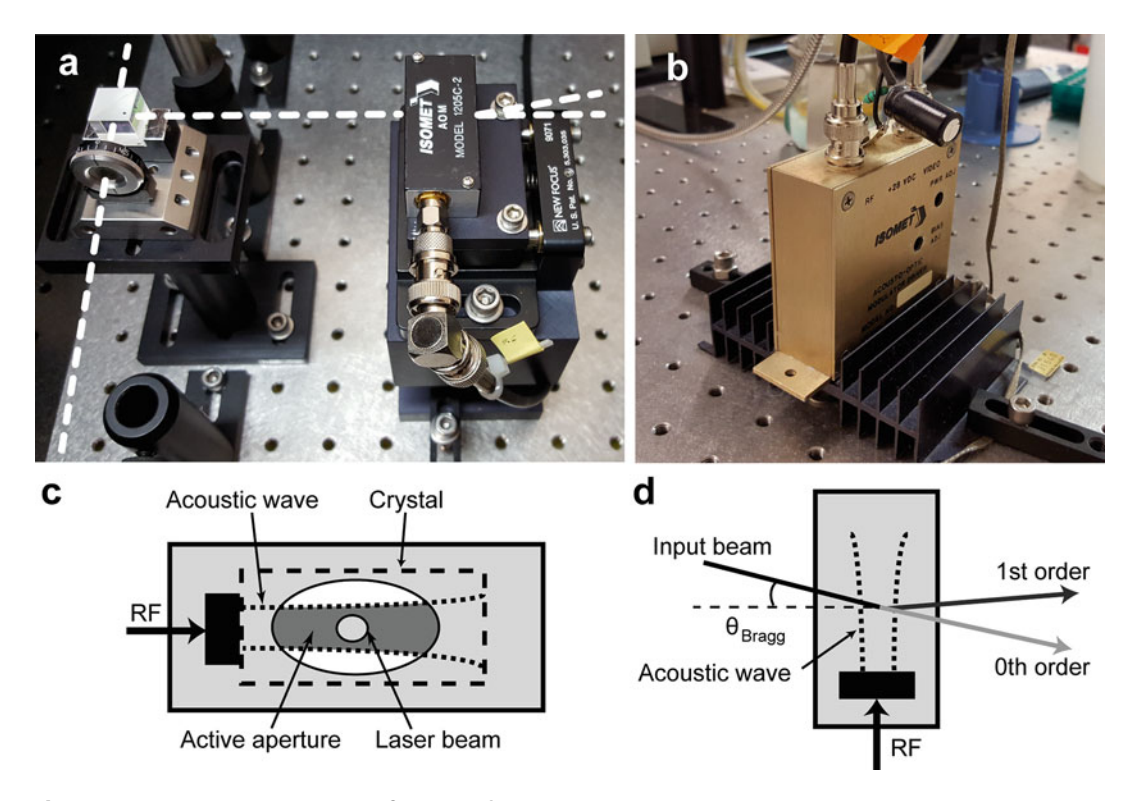


Fig. 3 (a) Photograph showing the AOM setup for the 1064-nm trapping laser (the *white dashed line* indicates the laser path). (b) Photograph showing the AOM driver with low-pass DC power filter and heat sink anchored to the optical table. (c) Cartoon depicting the operation of an AOM. The radio frequency (RF) voltage signal drives the transducer (*black*) to produce an acoustic wave in the attached crystal. The nodes and anti-nodes of the sound wave form a diffraction grating in the crystal. Note that changes in the acoustic wave's amplitude have to spatially propagate from the transducer to the far side of the laser beam to fully affect the first order beam's intensity. (d) Top view of the AOM's operation. Beams higher than first order are not shown, since they typically have very low intensity

- 2. Mount the AOM to the Tilt Aligner, and calculate the distance between the center of the AOM's aperture and the bottom of the Tilt Aligner stage. Call this distance y_A .
- 3. If y_0 and y_A are different, machine a monolithic block to serve as a mount for the Tilt Aligner and AOM. If necessary, a machine shop can help with this task. Make the block height $y_0 y_A$, so that the center of the AOM's aperture is located at the optical axis. The block should be machined so that it can be securely anchored using table clamps (e.g., Thorlabs, CL5) (Fig. 3a).
- 4. Machine or purchase a finned heat sink for the modulation driver. Our design is shown in Fig. 3b. Secure the driver to the heat sink using a thermal transfer paste, and clamp the heat sink down to the table.
- 5. Solder the power supply output to the "+Vdc" input of the driver. Connect the driver's "MOD" input to a controllable DC voltage source (note the "MOD" input has a 0–1 V range). Connect the "RF" output to the AOM.

3.2 Maximizing the Diffraction Efficiency of a Laser through an AOM

An AOM system can efficiently diffract incident laser intensity into the first order beam. Higher-order beams exist, but have very weak intensities. Our feedback design couples the first order beam into an optical fiber, because the intensity in the first order beam can be reduced to zero. Therefore, to make the most effective use of limited trapping laser power, we maximize the intensity of the first order beam. Diffraction Efficiency (DE) is the ratio of laser power in the first order beam when the RF power is on over the power in the zeroth order beam when the RF power is off. DE depends on the RF power applied to the AOM, the height and angle at which the beam enters the AOM, and the width of the beam inside of the AOM. For NIR lasers, the DE will increase with increasing RF power (though not always linearly). This power dependency is in contrast to visible wavelengths, where the DE decreases after some wavelength-dependent saturation power P_{sat} . The P_{sat} values for NIR wavelengths are past the safe-operating limit of the AOM.

DE is maximized when a laser enters the AOM in the center of its "active aperture" at a specific angle called the Bragg angle (Fig. 3c, d). The active aperture is defined as the exposed part of the crystal where the acoustic wave is present (as opposed to the material aperture, which is just the exposed part of the crystal), and is specified by the length of its shortest axis. The material and active apertures of the AOM are not in general the same, and any laser power that fails to pass through the active aperture is lost. Therefore, the incident beam diameter should not be larger than the short axis of the active aperture; DE is maximized when these two widths are equal. While smaller beam widths reduce the DE, they improve the rise time of modulations, since acoustic wave propagation across smaller beams takes less time (see Note 6). We set the beam width of our trapping laser equal to the active aperture to maximize DE. We kept the detection lasers at their initial beam widths, since their DE was not critical because only a few mW of laser power was needed. We angularly aligned the AOM by manually turning its mounting block until the DE was maximized. Finally, for aligning any near-IR laser, laser safety goggles should always be worn.

- 1. Turn the driver's "PWR ADJ" control screw all the way to the right, then back ¼ of a turn. If a "BIAS ADJ" control screw is present, turn it all the way to the left. These adjustments will increase the DE.
- 2. Find the active aperture specification in the AOM's data sheet, and measure your initial beam width.
- 3. For a trapping laser, determine the ratio in beam size needed to change the initial beam diameter to match the active aperture width and then calculate the pair of focal lengths needed to

achieve this change in beam size using a telescope. Install that telescopic lens system between the laser and the AOM. In general, this step can be skipped for detection lasers. For high-power lasers, be sure to check that the expected maximum laser intensity does not exceed the damage threshold of the AOM.

- 4. Install the half-wave plate, PBS cube, and beam block as shown in Fig. 1e, so that the majority of the light is directed into the AOM in a pure polarization state.
- 5. Use the half-wave plate to reduce the laser power into the AOM until its output beam (with the "RF" off) is barely visible on an IR detector card.
- 6. Read the power in the output beam with a power meter, and turn the half-wave plate back until the detected power is ~5 mW. Remember to work within the linear range of the power meter.
- 7. Turn on the power supply to the driver, and set the "MOD" input to an intermediate value (we use 0.4 V). Use the IR card to find the zeroth and first order beams, and move the power meter so that it only detects the first order beam (or simply block the zeroth order beam).
- 8. Slightly unclamp the AOM mount block so that it can be rotated. Slowly rotate the block and watch how the power in the first order beam changes. Clamp the block at the position that gives the largest power.
- 9. Perform the same alignment with the tilt aligner, and measure the final output power in the 1st order beam. Calculate the DE by dividing this value by the power you used in **step 6**.
- 10. For more detection sensitivity, turn the half-wave plate to increase laser intensity into the AOM. Then repeat **steps 6–9**. We typically align until the DE is above 0.75.

3.3 Coupling the First-Order AOM Diffraction into an Optical Fiber When a laser is coupled into a single-mode, polarization-maintaining optical fiber, its pre-fiber mode and pointing noise are converted into intensity noise (Fig. 2a, b). We couple the AOM's first order beam into such a fiber and use an AOM-mediated feedback loop to stabilize the post-fiber intensity noise. An angle-cleaved connector (FC/APC) at the fiber input mitigates back reflections, and a flat connector (FC/PC) at the fiber output ensures that the post-fiber beam emerges in a circular TEM₀₀ mode. To couple the laser into the fiber, we use an ultrastable, micro-positioning fiber coupler with an embedded focusing lens. The efficiency of this fiber coupling is maximized when the diameter of the collimated input beam *D* satisfies the following equation:

$$D = 2f(NA_{\text{fiber}}) = f\frac{4\lambda}{\pi\omega},\tag{1}$$

where f is the focal length of fiber-coupler lens, $NA_{\rm fiber}$ is the numerical aperture of the fiber ($NA_{\rm fiber} \equiv 2\lambda/\pi\omega = 0.11$ for $\lambda = 850$ nm), λ is the beam wavelength, and ω is the mode-field diameter (MFD) of the fiber at the laser wavelength. Note this $NA_{\rm fiber}$ is based upon the MFD, not the manufacturer's specified NA, which is typically 20–30 % larger. We use a 5-mm fiber coupler (f = 4.6 mm), and NIR fibers will typically have MFD values of 5–8 μ m.

The D value for maximum coupling efficiency will probably not equal the diameter needed for maximal DE in the AOM. Thus a two-lens telescope is needed to change the beam diameter. For trapping lasers, this two-lens system can also be used to mitigate the thermally induced pointing noise that arises from large RF power changes to the AOM. Specifically, when the modulation signal to the transducer changes, there is a transient temperature gradient in the AOM crystal that distorts the diffraction grating and leads to pointing noise in the diffracted beam [13]. A two-lens system reduces the severity of the thermally induced pointing noise so that the feedback loop can fully remove this adverse effect from the output beam. To determine the parameters for this system, a ray matrix equation for two thin lenses and two free-space propagations must be solved. Solving this matrix equation, one finds that:

$$D = d\left(1 + \frac{l_1 l_2}{f_1 f_2} - \frac{l_1 + l_2}{f_1} - \frac{l_2}{f_2}\right); \quad l_1 = f_1 + f_2, \quad (2)$$

where f_1 and f_2 are the focal lengths of the first and second lenses, l_1 is the distance between the two lenses, l_2 is the distance between the second lens and the fiber coupler lens, and d is the diameter of the beam before the first lens (ideally the same as the diameter in the AOM).

- 1. Block the zeroth order beam with either an iris (for milliwatt-scale beams) or a beam block (for watt-scale beams).
- 2. If the laser will only be used at a fixed intensity (such as the detection lasers), skip this step. For beams that require a dynamic intensity—namely the trapping beam—solve Eq. (2). D and d will be fixed, and the ranges of l_1 and l_2 will depend on the available space. We use $f_1 = 200$ mm and $f_2 = 300$ mm plano-convex lenses. Note that Eq. (2) does not need to be a strict equality, but differences should be kept below 20 %. Install the two lenses at their corresponding distances, putting the second lens on a translation stage.

- 3. Install two turning mirrors before the fiber coupler. We use these mirrors as a 2-mirror beam walk, to align the beam into the fiber coupler.
- 4. Screw the fiber coupler into one end of the fiber bench, and install the fiber bench half-wave plate.
- 5. Align the two turning mirrors such that the power through the half-wave plate and fiber coupler (without any patch cable attached) is maximized.
- 6. To make preliminary alignments to the fiber coupler, attach the patch cable to it, and attach a handheld fiber optic tester to the other end of the cable. A visible red laser should now run backwards through the system. Adjust the fiber coupler's five degrees of freedom such that the test beam overlaps the laser (going as far back upstream as possible). Note that a pair of irises uniquely defines a beam path. So by aligning both the visible and near-IR lasers to such a pair of irises, one can facilitate this process.
- 7. Remove the fiber-optic tester. Use a power meter to detect whether laser light is emerging from the cable's output connector; if there is no light, redo **steps 5** and **6**. Otherwise, adjust the fiber coupler screws slowly to maximize the transmitted power (*see* **Note 7**). A good alignment will give ~75 % or more transmission.
- 8. For trapping lasers, jump the AOM driver "MOD" voltage from a low value to a high value (e.g., 0.1 V to 0.6 V). Observe the intensity stability after the fiber in response to a large, abrupt change in RF power. If unacceptable, translate the position of the second lens along the *z*-axis—the laser propagation axis—so that *D* decreases, and try again. Iterate this process until you reach an optimum compromise between baseline fiber-coupling efficiency and pointing stability for your application. By changing the position of the lens, the diameter and cone-angle of the laser is altered at the fiber input. This process sacrifices coupling efficiency for stability in response to a large change in laser power induced by a change in the AOM.
- 9. When satisfied with the alignment, cover the fiber coupler with its dust cover and gently clamp a length of cable near the fiber coupler such that it does not sag or bend near the coupler (sharps bends reduce transmission efficiency). We use two machined blocks that can be screwed snuggly together, and have grooves down their middles in which the cable can securely sit. Figure 4a shows our finished fiber input setup.

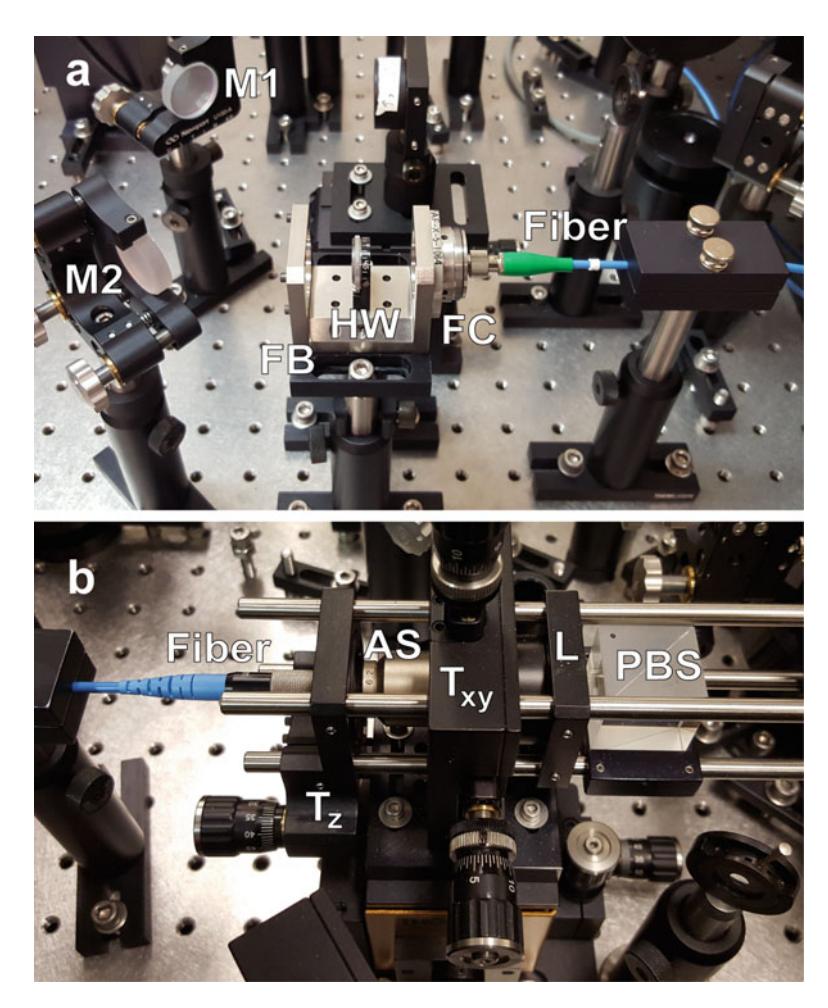


Fig. 4 (a) Photograph showing our setup for coupling a laser into an optical fiber. M1 and M2 are turning mirrors, FB is a fiber bench, HW is a half-wave plate, FC is a fiber coupler, and Fiber is a polarization-maintaining, single-mode optical fiber. (b) Photograph showing our fiber output setup. T_z is a fiber-cage Z translator, AS is an aspheric lens, T_{xy} is a fiber-cage XY translator, L is a plano-convex lens, and PBS is a polarizing-beam splitter

3.4 Launching the Laser and Monitoring the Fiber Output Intensity with a Photodiode

To launch the laser out of the fiber and feedback on its intensity for the stabilization feedback loop, we construct a fiber launch system that expands and collimates the fiber output beam (see Note 8). We use a stable multi-axis translation stage underneath to aid in subsequent beam alignment. Specifically, x and y motion of the fiber launch translation stage maps to pure rotations in the imaging plane of the microscope; z-axis motion of the fiber tip relative to an aspheric lens provides for fine control of laser collimation. A PBS cube in the fiber launch is used to re-polarize the laser after the fiber, since small rotations in polarization can occur over time, even with a polarization-maintaining fiber. The PBS cube turns this polarization noise into intensity noise, which is mitigated by the feedback loop. Figure 4b shows our finished fiber launch setup.

To measure the intensity of the laser after the fiber launch, we use a 90/10 beam sampler that diverts 10 % of the output laser intensity onto a photodiode. The photodiode's current signal is converted to a voltage that is input into an analog AOM-servo circuit board that, in turn, outputs a voltage signal to the AOM driver. The rest of the laser light is sent into a microscope objective to serve as either a trapping or a detection laser.

We use silicon analog photodiodes in a TO-36 packaging for all of our lasers (YAG-444AH). These photodiodes have a 60-MHz bandwidth and 5-ns rise time for a $50-\Omega$ load at $\lambda=1064$ nm when applying a large (-180 V) reverse bias. Reverse biasing eliminates a wavelength-dependent filtering in silicon photodiodes, including quadrant photodiodes, when using 1064-nm light [16]. By reducing the reverse bias, we tradeoff increased thermal stability of the photodiode during large-laser power changes for decreased detection bandwidth. We find that -30 V is a good compromise between signal stability and response time for this feedback loop (\sec Note 6).

- 1. Install a fiber-launch cage system on an optics table (we use the KT110 by Thorlabs). Put the FC/PC fiber adapter plate in the Z translator, and slide the mount onto the XY translator's back assembly rods. Make sure the adaptor plate's center is at your set optical-axis height y₀, and that its key slot is vertical (so that the output polarization is vertical). Connect the fiber optic patch cable (FC/PC end) to the adaptor plate.
- 2. Mount an aspheric lens into the XY translator, with the planar side facing the fiber's adaptor plate. We use a mounted aspheric lens with an anti-reflection coating (Newport 5723-H-B) and an RMS-threaded asphere adaptor (Newport 5709). We then use the RMS-to-SM1 adaptor ring from the fiber launch kit to install the aspheric lens into the XY translator.
- 3. Screw the SM1 iris diaphragm into the cage plate, and mount it on the assembly rods downstream of the XY translator. Open the iris fully, and slide it to the end of the cage assembly. Now adjust the distance between the Z translator mount and the aspheric lens so that the diverging output beam passes through the iris unclipped. Screw-tighten the Z translator to the assembly rods at this position. Remove the iris from the cage.
- 4. Determine the beam diameter you wish to send into the rest of the optical-trapping setup. Call this diameter d_0 . A planoconvex lens needs to be added to the cage assembly to collimate the fiber output beam to this diameter. To determine the required focal length for this lens, measure the beam diameter at a position close to the XY translator (using either a beam profiler or a razor blade and power meter). Use a ruler and a piece of tape to mark the location of this measurement on the optics table. Repeat this process at a position farther away from the translator. Call the smaller beam diameter d_1 , the larger

diameter d_2 , and the distance between them Δz . If we imagine the beam emerging from the XY translator as a cone of light from a point source, simple geometry says that θ , the angle between the optical axis and the cone's edge, must obey $tan(\theta) = (d_2 - d_1)/2\Delta z$. From here, a ray matrix calculation shows that the focal length needed to collimate the beam at diameter d_0 is $f = d_0/2\theta$.

- 5. Add this lens to the cage system at the location that collimates the beam. Install a PBS cube after the lens, so that polarization noise introduced by the fiber is turned into intensity noise and mitigated (*see* **Note 9**).
- 6. Place a 90/10 beam splitter after the cube. If the power in the 10 % beam is larger than 1 mW, install a reflective neutral-density filter to reduce the incident power.
- 7. Machine or purchase a photodiode mount that can screw into the XY translator. Install the photodiode into the mount, with a line filter placed in front of the photodiode at the laser's wavelength. Machine a protective casing with two BNC connectors to house the photodiode mount and a $10\text{-k}\Omega$ trans-impedance amplifier.
- 8. Assemble transimpedance amplifier based on the provided circuit diagram (*see* https://jila.colorado.edu/perkins/research/resources). Connect the photodiode's current output to the trans-impedance amplifier (to turn it into a voltage), and connect the amplifier to one of the two BNC connectors. Connect the photodiode's bias input to the other BNC connector, and attach to the photodiode's power supply. Install the photodiode into an XY translator and align the photodiode in the 10 % beam path (*see* Note 10).

3.5 Completing the Feedback Loop with an AOM Servo Board and Checking Performance The final component of the intensity stabilization feedback loop is a proportional-integral servo circuit board. This board takes the photodiode voltage and a user-determined reference voltage as inputs, and outputs a voltage to the AOM driver's "MOD" connector. The board tries to keep the photodiode voltage equal to the reference voltage by changing the AOM driver's modulation voltage. For example, if the photodiode voltage is above the reference, the board lowers the modulation voltage to decrease the DE of the AOM and thereby lowers the incident power on the photodiode. The parts list, schematic, and circuit board layout for this AOM servo board can be found at https://jila.colorado.edu/perkins/ research/resources, and this circuit board layout can be sent out for manufacture (e.g., at PCB Unlimited). The board is designed to fit into a single slot NIM case, and we use a NIM bin rack as its ± 15 V power supply. Once built, the servo board must be tuned to maximize its low frequency gain and minimize its gain at frequencies larger than the inverse of the AOM's response time. If the gain in that bandwidth is not zero, the servo loop will try to servo itself and will start oscillating.

- 1. Assemble the circuit board using the schematic, circuit-board layout, and parts list. Install into a single-slot NIM case. Power the board with ± 15 V (*see* Note 11).
- 2. Connect the photodiode's output to "PD INPUT (J13)," connect a cable carrying 5 V DC to "COMPUTER /INTERNAL CONTROL (J10)," connect "OUT TO AOM (J50)" to the AOM driver's "MOD" input, and connect "COMPUTER (EXTERNAL) INTENSITY CONTROL (J12)" to a controllable DC-voltage source. The laser-intensity servo loop is now complete.
- 3. Use a T-connector to simultaneously read the "PD INPUT" on a real-time spectrum analyzer (1-MHz bandwidth), and turn the coarse gain, fine gain, and PI corner controls all the way counter-clockwise (*see* Note 12).
- 4. Set "INTENSITY CONTROL" to a low voltage (such as 1 V), and see whether the green board LED lights up. If it does, the servo loop is working and "locked" at the set voltage. If the "under" LED lights up, the photodiode's voltage is less than the reference. Check your optical system to make sure laser light is making it through the fiber, and onto the photodiode. If the "over" LED lights up, the photodiode voltage is larger than the reference, and the servo is trying to reduce the power in the AOM's first order beam. If the "over" status persists, check the optics and try turning the power to the board and AOM driver off and on.
- 5. Once the servo is locked, turn the coarse gain up until the signal on the spectrum analyzer starts to peak, then back down one notch. Do the same for the fine gain, turning it back half a screw turn, and repeat for the PI corner. The servo is now tuned. If a spectrum analyzer is not available, this procedure can be done with an oscilloscope where the signal will start to oscillate with too much gain.
- 6. The best way to check the performance of a feedback loop is to monitor the control variable using an out-of-loop detector. To check this servo's performance, take another beam sampler and monitor the fiber output intensity on a second, out-of-loop photodiode, as shown in Fig. 2b. A plot of normalized laser intensity vs. time when the servo is off (gray) and on (black) is shown in Fig. 2c.

3.6 Cleaning Glass Coverslips

To stabilize the position of the sample surface, we fabricate fiducial marks onto the surface, monitor their position with a detection laser, and counter any observed drift with a three-axis PZT stage. Before fabrication begins, the coverslips must first be cleaned.

We use the following protocol for typical glass cleaning, and O_2 plasma if more rigorous cleaning is needed. Note that a base-etch, such as KOH, should not be used to clean the coverslips *after* fabrication, as it will etch the HSQ posts off of the glass.

- 1. Use a diamond scribe to write a small "X" into the lower right corner of each of the coverslips (on one side only). This will be the side onto which we fabricate fiducial marks.
- 2. Place 80 g of potassium hydroxide (KOH) pellets and 250 mL of completely denatured ethanol into a 1-L beaker, and dissolve using a magnetic stir bar and plate (*see* **Note 13**). This gives a 5.7 M KOH solution.
- 3. Place this beaker into an empty ultrasonic bath. Place two half-filled 1 L beakers of filtered (0.2 μ m) water and one 1 L beaker of 300 mL acetone in the bath, as well, for a total of four beakers.
- 4. Fill the ultrasonic bath with water (up to 3 in. high), and turn on
- 5. Load coverslips into a Teflon coverslip rack (shown in Fig. 5a) and submerge into acetone solution for 3 min.
- 6. Rinse coverslips and rack with ethanol, and then submerge into the KOH solution for 3 min.
- 7. Rinse all of the KOH solution off with filtered water, and submerge into the first beaker of water for 3 min.
- 8. Rinse again with filtered water, and submerge into the second beaker of water for 3 min.
- 9. Rinse with filtered water and then with ethanol. Dry the ethanol-rinsed coverslips and rack by placing them into a microwave for 2 min on high heat.
- 10. Store in a sealed container, such as an empty pipette tip box with Parafilm covering.

3.7 Fabricating Fiducial Marks onto Coverslips We fabricate fiducial marks onto coverslips using a hydrogen silsesquioxane (HSQ) negative resist and e-beam lithography. HSQ crosslinks to form a low-index glass when exposed to EUV or e-beam radiation, and non-cross-linked HSQ can be removed from glass using tetramethylammonium hydroxide (TMAH). To make fiducial marks, we therefore spin-coat a coverslip with a 0.4–1-µm thick layer of HSQ, and then e-beam pattern an array of ~600-nm diameter circular dots onto the HSQ layer in a low-vacuum environment. The excess, non-irradiated HSQ is then removed (i.e., "developed") using a solution of TMAH and water. This procedure creates an array of glass posts covalently attached to the coverslip, as shown in Fig. 5b. Other fabricated fiducial marks, such as silicon disks, can also be used, as detailed in a previously published protocol [17]. Non-fabricated fiducial marks, such as beads stuck or

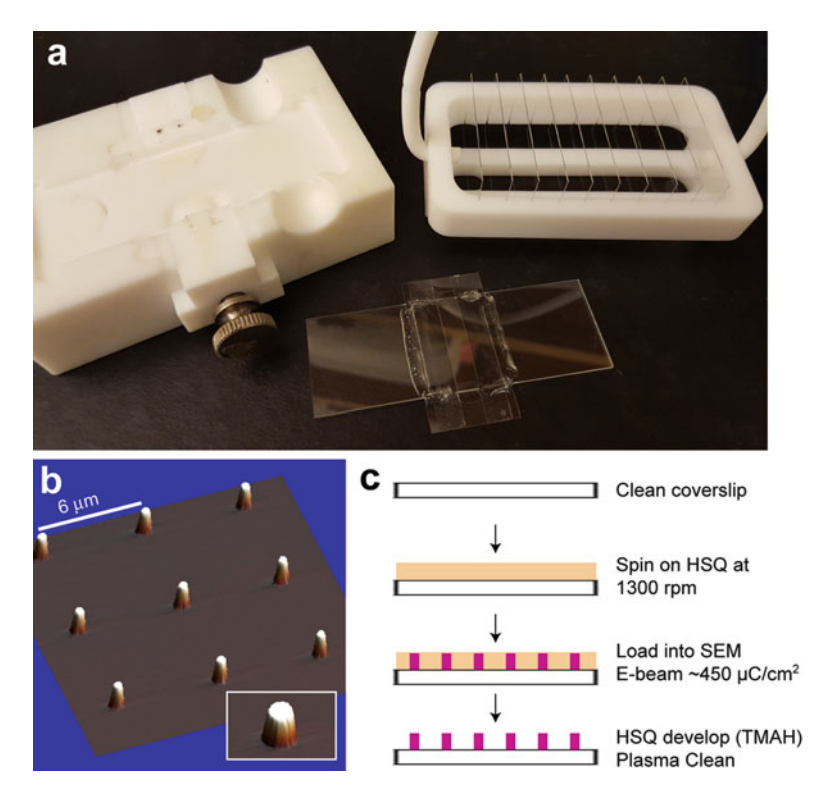


Fig. 5 (a) Photograph showing a custom-machined Teflon block for reproducibly placing coverslips containing fiducial marks onto a microscope slide (*left*), an example flow cell (*middle*), and a Teflon rack and handle for cleaning coverslips in acids or bases (*right*). (b) Atomic-force-microscope image of a coverslip surface patterned with fabricated fiducial marks. Note these posts are spaced 6 by 6 μ m apart. Optimum spacing depends on the length of DNA, the size of the bead, and the range of the electronically steerable mirror. We often use a 15- μ m spacing for 2- μ m long DNA when using 0.7- μ m diameter beads. (c) Cartoon of the fiducial mark fabrication process

melted onto the surface, will, in general, not suffice for Å-scale stabilization [12], since they are not covalently attached to the surface and typically move relative to the coverslip with >1 Å motion. Such motion tends to get worse after multi-hour exposure to an aqueous environment.

This procedure requires the use of a spin coater, an O₂-plasma reactive-ion etcher, and a scanning-electron microscope (SEM) with a low-vacuum sample chamber (to prevent harmful charging effects, *see* **Note 14**). Such equipment is often housed in shared clean room facilities, with different models having different capabilities and limitations. Since your equipment will most likely differ from ours, we provide only general instructions for this part of the protocol. Likewise, the fabrication parameters given below were optimized for our specific equipment; treat our values as

representative ones from which to start your own optimization process.

- 1. Design an automated SEM procedure to pattern a $1.5 \times 1.5 \text{ mm}^2$ area in the center of the coverslip with 600-nm diameter dots, spaced 15 µm apart vertically and horizontally. We use DesignCAD and NPGS software for this purpose, with the following parameters: dosage = $450 \,\mu\text{C/cm}^2$; current = $25 \,\text{pA}$; center-to-center = $6.82 \,\text{nm}$; line spacing = $50.02 \,\text{nm}$; magnification = $1000 \times$.
- 2. Prepare a coverslip for spin coating by placing it on a 200 °C hotplate for 2 min, diamond-scribed side up. Ensure that in all subsequent steps, the coverslip is always placed scribed side up.
- 3. Place the coverslip onto the spinner and pipette $200 \, \mu L$ of HSQ (FOx 16) onto it. Spin at $1000{\text -}5000 \, \text{rpm}$ for 50 s at an acceleration of 5.5 krpm/s to make $0.4{\text -}1{\text -}\mu \text{m}$ tall posts ($1000 \, \text{rpm}$ makes $1{\text -}\mu \text{m}$ -tall posts).
- 4. Post-heat the coverslip on a hotplate at 180 °C for 4 min.
- 5. Load the coverslip into the SEM and pump the sample chamber down to low vacuum [0.075–1 Torr (10–130 Pa)]. Ensure that a low-vacuum detector (LVD) is in place. Set voltage to 30 keV, align and focus the SEM, and run your exposure program.
- 6. Once the program is complete (~20 min), turn off the voltage and bring the chamber to atmosphere.
- 7. In the fume hood, fill a 1 L beaker with the TMAH development solution CD-26 (enough to comfortably submerge the coverslip), and fill another 1 L beaker with distilled water. Using tweezers or a Teflon coverslip holder, submerge the coverslip in the TMAH solution for 12 min., then remove and immediately submerge in the distilled water beaker for 1 min.
- 8. Remove coverslip, rinse off with filtered-water squirt bottle, and dry with nitrogen gas. Use a microscope capable of observing micron-scale features to check whether development is complete. If not, repeat step 8.
- 9. Once the coverslip is completely developed, it must be cleaned in an O₂-plasma etch. We perform our etch in a PlasmaSTAR etcher at <25 mTorr (3 Pa) vacuum with the mass-flow controller set to 100 sccm and the power set to 550 W. At these conditions, we run two 180-s etches. Between etches we rotate the metal holder containing the coverslip.

3.8 Assembling Flow Cells with Fabricated Coverslips

The single-channel flow cells we use have a simple design and can be made by hand in a few minutes. They have dimensions of $25 \times 5 \times 0.15$ mm³ corresponding to a 15-µL volume. More

complicated microfluidic designs exist [18], and can be integrated with coverslips containing fiducial marks. Fig. 5a shows a finished flow cell.

- 1. Place a microscope slide onto a clean surface. This can be a simple tabletop, or something more complicated like a machined Teflon mount (*see* Fig 5a). Such a mount improves the repeatability of flow cell construction by having pre-marked locations for tape and coverslip placement (*see* steps 3 and 4), ensuring that the post array is located in the same part of the microscope slide, and thus can be easily located under the microscope.
- 2. Take a ~5-cm-long piece of double-sided tape and stick it lengthwise by its edge to the top edge of the table. Use scissors or a razor blade to cut the tape in half.
- 3. Take the two tape halves and stick them onto the slide, perpendicular to the slide's long axis, 5-mm apart.
- 4. Take a fabricated coverslip from Subheading 3.8 and lay it mark-side down on the two tape halves, again perpendicular to the slide's long axis. Make sure the fiducial mark array is centered and that the coverslip overhangs the slide on both sides equally. Using the tip of a Pipetman (or something similar), gently press the coverslip into the tape to ensure a firm, uniform bond (*see* Note 15).
- 5. Use a razor blade to cut off any tape overhanging the coverslip.
- 6. Repeat the above steps until you have the number of flow cells you plan to use that day.
- 7. To rigidify the flow cells, mix together 5-min epoxy in a disposable cup and apply it to the gaps between the coverslip and the slide (except for the fluid channel). Pipette tips are our preferred tool for this task.

3.9 Processing a QPD Voltage Signal with an Offset Amplifier Circuit Board Back-focal-plane detection is widely used to measure bead motions in an optical trap from a change in light distribution on a quadrant photodiode (QPD) [5], either directly with the trapping laser or with a weaker detection laser. To process the voltage signal from a QPD, we use electronics to amplify the normalized difference signals (typically referred to as V_x and V_y) and to offset-amplify the sum signal, the total light falling on the QPD (V_z). By calculating a normalized difference signal, the lateral motion is approximately independent of laser intensity variations. However, since vertical motion of the bead or the fiducial mark is detected as a change in the total light incident upon the QPD, variations in the laser intensity used to detect such vertical motion is indistinguishable from actual vertical motion. Indeed, a variation in intensity of just 1 % appears as ~30-nm-scale axial motion. Additionally, these

small voltage changes make it difficult to precisely measure axial motion. Hence, we amplify the initial QPD's sum signal (V_z) by $g(V_z-V_0)$, where g is the gain and V_0 a fixed offset voltage. The resulting amplification leads to a larger signal variation per unit displacement (i.e., the sensitivity in V/nm). To do this, we use an analog offset-amplifier to match the variable portion of the sum signal to the ± 10 -V range of a standard 16-bit data-acquisition (DAQ) system. For simplicity, we also refer to the offset-amplified sum signal as V_z .

- 1. Use the schematic and parts list provided at https://jila.colo rado.edu/perkins/research/resources to assemble the offset amplifier, and install it into a single slot NIM case. Power the board with ± 15 V (see Note 11).
- 2. If necessary, install a data-acquisition system. Split the QPD signals into V_x , V_y , and V_z components, and send them through an anti-aliasing filter set to half of your data-acquisition system's sampling frequency. Send the resulting z signal into an offset amplifier, and then all three signals into the DAQ system.
- 3. Test that the system can collect voltages from the QPD, process them, and record them onto a computer.

3.10 Preparing the Instrument for Surface Stabilization Since it is outside the scope of this chapter to detail the installation of common optical-trapping components, this section and all following sections will assume that the experimenter has: installed two detection diode lasers and one trapping laser, and stabilized them using the methods of Subheadings 3.1-3.5, installed computercontrollable 2-axis PZT mirrors (or equivalent beam-steering optics) in the trapping and detection lasers' beam paths, combined beam paths of all three lasers, coupled the lasers into an objective lens, installed a condenser lens and three QPDs to collect the scattered and transmitted laser light from the sample plane, projected a visible light source into the sample plane, and installed a CCD camera and monitor to image the sample plane. In addition, we will not cover the common passive-stabilization techniques used to mitigate environmental noise [5, 6, 19]. These include: enclosures for all optical components, mounting all optics on vibrationisolation tables, housing the instrument in a temperaturestabilized, acoustically quiet room (we use NC30), and mechanically stabilizing instrument components to reduce their susceptibility to environmental vibrations.

1. Connect and install the PZT stage and controller into the existing optical-trapping setup. Be sure to mechanically stress relieve the cable from the controller to the PZT stage, so inadvertent cable motion (i.e., swinging) does not introduce mechanical noise. We use a Nikon TE2000-S inverted

- microscope. Alternative trapping designs in the absence of a commercial microscope frame are also used [20].
- 2. Connect the stage controller to a computer. The three communication protocols are available for our PZT stage: serial (RS-232), GPIB (IEEE-488.2), and PIO. We find that GPIB suffices for most applications (*see* Note 16). Stage manufacturers typically provide LabVIEW software for communicating with the controller. Install that software and ensure its functionality.
- Install a microscope slide adaptor plate that screws into the top of the piezo stage. Read the stage manual carefully for proper installation procedures, as screws that are too long can damage the stage.
- 4. Mount the sample slide into the holder, and align the objective and condenser lenses.
- 5. Focus the objective until the CCD camera's imaging plane aligns with the sample surface. If the center of the fabricated sample cell is aligned with the objective's field of view, you should see a regular array. If not, adjust the lateral position of the sample.
- 6. Next, the focus of each laser beam must be appropriately placed in space. To set the vertical position of the trap relative to the imaging plane, first fill the sample chamber with a dilute solution of beads. Trap a bead, and then move the stage in z until the coverslip contacts the bead (which can be detected by an abrupt change in the trap's QPD z voltage signal [21]). We then change the collimation of the trapping laser beam until the sum signal (V_z) of the bead does not change when retracting the trapped bead away from the coverslip surface by changing the vertical position of the stage. Nonideal collimation will result in a V_z signal that drops linearly in z (note, in both cases, Vz is modified by oscillatory Fabry-Perot interference [21]). Collimation of the trapping beam is adjusted by changing the position of the tip of the single-mode fiber (as detailed in Subheading 3.4). We then move the position of the CCD camera to bring the image of a trapped bead into focus.
- 7. The vertical position of the detection lasers' foci should be set to maximize their detection sensitivity (in V/nm). To this end, we vertically position the bead detection laser's focus ~50 nm past the beam waist of the trap laser so that the detector beam focus is in the center of the trapped bead (which is displaced past the trapping beam waist due to radiation pressure). The fiducial mark detection laser is most sensitive when its beam waist is centered vertically with respect to the post. In our setup, the post detection laser's beam waist is ~400 nm upstream of the trap's focus (i.e., closer to the surface).

- 8. With the *z* positions of the lasers set, move the post detection beam onto a nearby post using the manual turnscrews of the PZT mirror. If the low-power detection beam cannot be imaged in the water-filled cell, use real-time voltage readings from the QPD to tell when the beam passes over a post. Generally, a color filter can be positioned in front of the CCD camera to attenuate the trapping-beam wavelength but still allow visualization of the much weaker detection lasers.
- 9. LabVIEW software is used to precisely center the beam over a post. To do so, we use a closed-loop tip-tilt PZT mirror to electronically steer the laser across the post in the x and y directions (±300 nm), while its QPD voltages are recorded as a function of beam position. The resulting signals are nearly the derivatives of Gaussians, with the center of the post corresponding to the lateral center point of this function: its antisymmetry point. We therefore fit a derivative of a Gaussian to each of these signals, and extract the fit parameters. One of those parameters is the "center offset," the distance between the antisymmetry point (the post's center) and the center of the scanned range. We convert that position into a PZT voltage and use it to reposition the beam's PZT mirror, centering the beam. We typically repeat this process again to fine-tune the position (see Note 17).

3.11 Coding a
Surface-Stabilization
Feedback Loop and
Testing Final
Performance

To complete the surface-stabilization feedback loop, we use a Lab-VIEW program to monitor the surface position and move the PZT stage to compensate for any unwanted surface movement. We first calibrate the detector so that V_x , V_y , and V_z can be converted to the x, y, and z spatial positions of the post. Once that is done, we choose a set position $(x_{set}, y_{set}, z_{set})$ for the post. We then continuously measure the post's position. Every 10 ms (100 Hz bandwidth), the program computes the mean current position of the post over the previous 10-ms window and takes the difference between this measurement and the set position. The software-based feedback loop then moves the stage a portion of that difference in the opposite direction (we use -0.2 as our proportionality constant). More complex control schemes, such as differential or integral feedback, are also possible, but we find that proportional control is enough to stabilize the surface to 1 Å in 3D over 1-s intervals (1-25 Hz bandwidth) and keep the drift sub-nm over 50-s intervals [12].

The resonance frequency of the PZT stage limits how fast this feedback loop can operate. For our PI P-517.3CD, it is ~500 Hz. Hence, the minimum loop closure time is ~2 ms. The response time of the stage to software commands also affects the loop closure time, but the software can be tuned to minimize this delay. A more robust (though more complex) version of this stabilization can be found in ref. [22], which achieves 1 Å in 3D stability over 1000 s.

The best way to test the performance of a feedback loop is to measure the control variable using an out-of-loop detector. To that end, we routinely test the performance of the surface-stabilization loop by monitoring the position of a second fiducial mark on the surface with a second, out-of-loop detection laser (Fig. 6a). This gives us a much more accurate measure of stability, since noise sources hidden from the feedback loop (such as positional drift of the in-loop laser) can be measured. Using this out-of-loop laser test, we find that the ultimate limit on our stability is set by the differential-pointing stability between the lasers.

- 1. Once a detection beam is centered over a post (*see* Subheading 3.9), the voltage output from the detection electronics must be calibrated into a position. To calibrate the voltage signal, scan the post through the laser focus in all three axes using the stage. Record the stage position vs. detected voltage curve for each axis. Fit a seventh order polynomial to each curve, *using voltage as the independent variable*, and extract the eight fit coefficients. These coefficients are our calibration. To go from detected voltage to post position, just form a voltage polynomial with these coefficients and take the sum. We typically scan ± 200 nm in 1-nm steps, and for each step average 30 points taken at 4000 Hz.
- 2. For the stabilization algorithm, create a while loop that performs buffered continuous data acquisition on the position of the post. We take 1200 samples per iteration at 120 kHz and average them, giving us a loop update time of 10 ms.
- 3. At the start of the while loop, store the initial post position as the "Set Position." Every following iteration, take the difference between the current position and the set position. Multiply that difference by -0.2 and send a move command to the stage controller to move the stage by that amount. Let this while loop run during your experiment, and algorithmically or manually stop it when you are finished.
- 4. To test stabilization performance, modify the above program so that a second out-of-loop detector beam can simultaneously measure the position of a second post. Center that beam over the post, scan the post through the beam so that its voltage signal is calibrated, and then perform the same data acquisition. Results from this kind of experiment are shown in Fig. 6b, c.

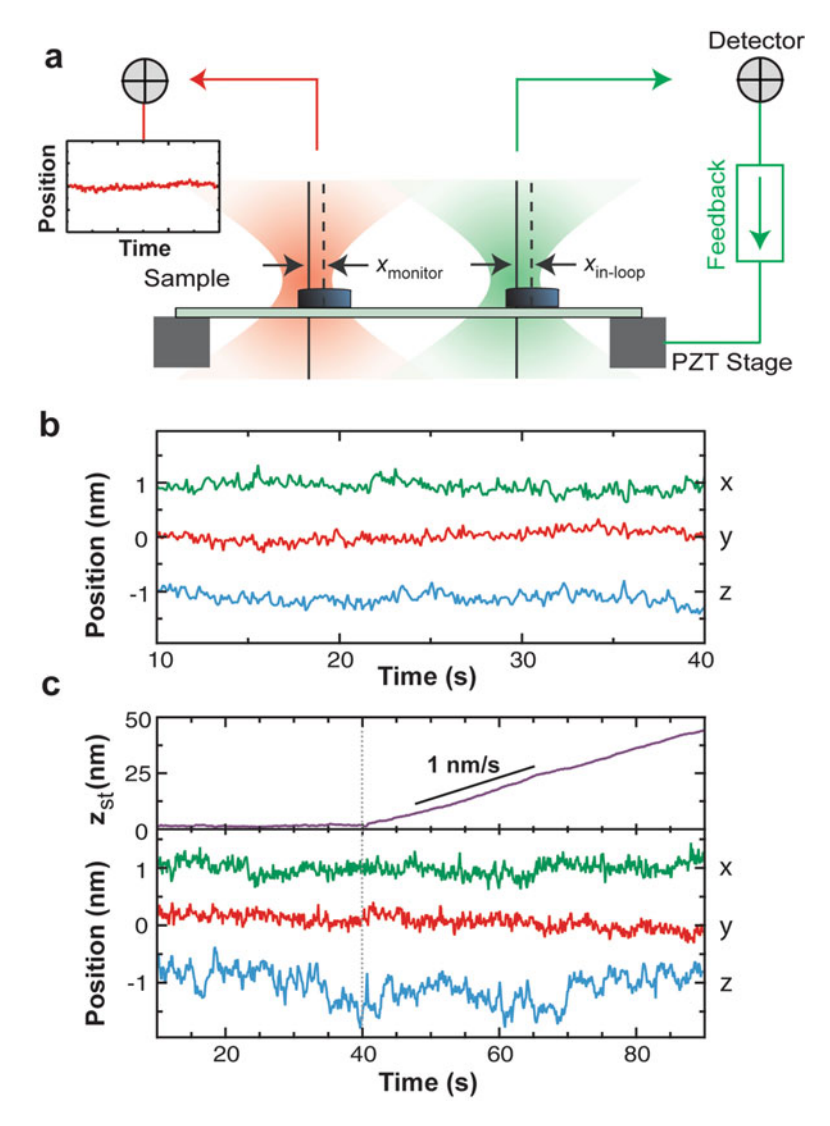


Fig. 6 (a) Diagram for characterizing the performance of the surface-stabilization feedback loop using an out-of-loop detector. Note that any well-performing feedback loop necessarily drives the in-loop signal to zero over long timescales. Hence, characterizing sample stability based on an in-loop measurement leads to incorrect conclusions. For instance, it cannot distinguish laser-pointing noise from lateral sample motion. (b) Sample position vs. time measured by the independent, out-of-loop laser. Traces offset from zero for clarity; x: top trace, y: middle trace, z: bottom trace. (c) As in (b), but at t=40 s, the intensity of the trapping laser was increased from 50 to 150 mW, leading to heating and expansion of the objective. The stabilization feedback loop compensated for this significant vertical drift by moving the stage in z (top curve). RMS stability in the short term (1 s) remained 1 Å, while long term RMS stability (50 s) was 1.5 Å in x and y, 2.6 Å in z (reprinted with permission from ref. [12]; © 2007 The Optical Society)

4 Notes

- 1. There are excellent video-based methods for stabilizing a microscope sample surface with nm precision [23]. Our laser-based technique is best suited to those applications that require sub-nm stability.
- This data-acquisition system is the one we currently use for our instrument, but less expensive options are available which will work just as well for the stabilization protocols detailed in this chapter.
- 3. A more detailed explanation of these components and how they function can be found in the support section of Isomet's website at isomet.com/appnotes.html.
- 4. Adding a low-pass filter to this connection can help filter stray AC signals.
- 5. It is helpful to use a calibrated standard, such as a post-mounted iris, to set height y_0 . With this standard, one can easily check whether a new optical element keeps the laser propagating at constant height y_0 .
- 6. The time it takes for a sound wave to propagate from the transducer to the far side of the laser beam is the ultimate limit in the response time of the servo loop. We find that the response time at 2-mm beam diameter is small enough for our optical-trapping purposes (giving us a ~200 kHz servo bandwidth).
- 7. Fiber-coupler alignment can be a tedious and frustrating process; this coupler was chosen for its stability, not its user friend-liness. Align the coupler in *x* and *y* first, and then leave those screws fixed. Optimize the positions of the three *z* screws one at a time. One of the *z* screws should improve the coupling much more than the others: this screw tilts the fiber coupler to accommodate the angle-cleaved fiber connector. Note that slightly adjusting the two turning mirrors during this alignment can provide surprisingly large results.
- 8. Our setup uses an aspheric lens and plano-convex lens to quickly collimate and expand the beam within a cage system. Other optical elements, such as triplet collimators, now exist which can perform the same task using only one component [24]. The cost of this simplicity is a loss of customizability and ease of access.
- 9. The reflectivity of dichroic mirrors is polarization dependent. If dichroic mirrors are used to combine multiple lasers beams into a single-beam path (as widely done in many optical-trapping setups), any polarization noise in the incident beam will be transformed into intensity noise when it reflects off of the

- dichroic mirror. This source of noise is mitigated by the PBS cube and the intensity feedback loop.
- 10. Depending on the size of the incident beam, you may need to install an iris before the photodiode. The edge of the silicon chip is typically inhomogeneous, so it is good practice to not use this area for sensitive readings. An iris will also block any stray beam reflections from reaching the photodiode. A lens can help minimize the diameter of the beam before reaching the PD.
- 11. We position the power supply 1–2 m away from the board, after finding stray fields generated by the power supply coupled into the board's electronics and produce unwanted line (60 Hz) noise. Albeit very small (~90 nV), this noise is especially deleterious since it coupled into the reference voltage used in the offset-amplifier, where the small noise was multiplied by a large gain and inferred as vertical motion.
- 12. PI corner is technically a misnomer in this design. The corner is actually between a single integrator (20 dB/decade) and a double integrator (40 dB/decade).
- 13. We have found it difficult to completely dissolve KOH pellets with more than 0.4 % potassium carbonate content.
- 14. An alternative way to prevent charging of an insulating substrate is to cover the substrate with a thin film of metal; we did this in early versions of the protocol. Specifically, we thermally evaporated a 15-nm layer of aluminum onto the resist, used the SEM to expose dots as usual, and then etched off the aluminum by soaking it in a solution composed of 80 mL phosphoric acid, 5 mL acetic acid, 5 mL nitric acid, and 10 mL distilled water for 10 s. After rinsing the coverslip with distilled water and nitrogen drying, we developed as usual.
- 15. We colloquially refer to this technique as "coloring in the slide," since a firm bond will make the tape look darker. If the slide is not colored in, fluid in the channel can leak out through the air gaps between the tape and one of the glass surfaces. Also color the tape that overhangs the slide on one side of the coverslip, to make sure that fluid does not leak between the tape and the glass during buffer exchanges.
- 16. Faster communication can be achieved by using a protocol based on a field-programmable gate array (FPGA), as demonstrated in ref. [25].
- 17. If after centering the laser precisely with respect to the post, you move a post in z through the laser focus and observe large voltage changes in x and y, the beam is tilted with respect to the z-axis of the stage. Adjust the XYZ translator that is supporting the full fiber launch system from Subheading 3.4 to align the

optical axis to the z-axis of the stage, and so reduce this cross talk. Note this is not the same as moving the XY-position of the aspheric lens with respect to the fiber tip, which would not have the desired effect.

Acknowledgments

We thank Carl Sauer for providing detailed electronic diagrams and associated files for the circuit boards. This work is supported by a National Science Foundation Graduate Research Fellowship (Grant No. DGE 1144083 to S.R.O.), a National Institute of Health Molecular Biophysics Training Grant awarded to S.R.O. (T32 GM-065103), the NSF (Phys-1125844), and NIST. Mention of commercial products is for information only; it does not imply NIST recommendation or endorsement, nor does it imply that the products mentioned are necessarily the best available for the purpose. T.T.P. is a staff member of NIST's quantum physics division.

References

- Svoboda K, Schmidt CF, Schnapp BJ, Block SM (1993) Direct observation of kinesin stepping by optical trapping interferometry. Nature 365:721–727
- Finer JT, Simmons RM, Spudich JA (1994) Single myosin molecule mechanics: piconewton forces and nanometre steps. Nature 368:113–119
- 3. Abbondanzieri EA, Greenleaf WJ, Shaevitz JW, Landick R, Block SM (2005) Direct observation of base-pair stepping by RNA polymerase. Nature 438:460–465
- Wen JD, Lancaster L, Hodges C, Zeri AC, Yoshimura SH, Noller HF, Bustamante C, Tinoco I (2008) Following translation by single ribosomes one codon at a time. Nature 452:598–603
- 5. Visscher K, Gross SP, Block SM (1996) Construction of multiple-beam optical traps with nanometer-resolution position sensing. IEEE J Sel Top Quant Electron 2:1066–1076
- 6. Neuman KC, Block SM (2004) Optical trapping. Rev Sci Instrum 75:2787–2809
- 7. Moffitt JR, Chemla YR, Smith SB, Bustamante C (2008) Recent advances in optical tweezers. Annu Rev Biochem 77:205–228
- 8. Lee W, Strumpfer J, Bennett V, Schulten K, Marszalek PE (2012) Mutation of conserved histidines alters tertiary structure and

- nanomechanics of consensus ankyrin repeats. J Biol Chem 287:19115–19121
- Perkins TT (2014) Angstrom-precision optical traps and applications. Annu Rev Biophys 43:279–302
- Pralle A, Prummer M, Florin E-L, Stelzer EHK, Horber JKH (1999) Three-dimensional high-resolution particle tracking for optical tweezers by forward scattered light. Microsc Res Tech 44:378–386
- 11. Denk W, Webb WW (1990) Optical measurement of picometer displacements of transparent microscopic objects. Appl Opt 29:2382–2391
- Carter AR, King GM, Ulrich TA, Halsey W, Alchenberger D, Perkins TT (2007) Stabilization of an optical microscope to 0.1 nm in three dimensions. Appl Opt 46:421–427
- 13. Carter AR, Seol Y, Perkins TT (2009) Precision surface-coupled optical-trapping assays with 1 base-pair resolution. Biophys J 96:2926–2934
- 14. Wang MD, Yin H, Landick R, Gelles J, Block SM (1997) Stretching DNA with optical tweezers. Biophys J 72:1335–1346
- 15. Shaevitz JW, Abbondanzieri EA, Landick R, Block SM (2003) Backtracking by single RNA polymerase molecules observed at near-base-pair resolution. Nature 426:684–687
- Peterman EJG, van Dijk MA, Kapitein LC, Schmidt CF (2003) Extending the bandwidth

- of optical-tweezers interferometry. Rev Sci Instrum 74:3246–3249
- 17. Paik DH, Perkins TT (2012) Single-molecule optical-trapping measurements with DNA anchored to an array of gold nanoposts. Methods Mol Biol 875:335–356
- 18. Candelli A, Wuite GJL, Peterman EJG (2011) Combining optical trapping, fluorescence microscopy and micro-fluidics for single molecule studies of DNA-protein interactions. Phys Chem Chem Phys 13:7263–7272
- 19. Bustamante C, Chemla YR, Moffitt JR (2008) High-resolution dual-trap optical tweezers with differential detection. In: Selvin PR, Ha T (eds) Single-molecule techniques. Cold Spring Harbor, New York
- Moffitt JR, Chemla YR, Izhaky D, Bustamante C (2006) Differential detection of dual traps improves the spatial resolution of optical tweezers. Proc Natl Acad Sci U S A 103:9006–9011

- 21. Neuman KC, Abbondanzieri EA, Block SM (2005) Measurement of the effective focal shift in an optical trap. Opt Lett 30:1318–1320
- 22. Walder R, Paik DH, Bull MS, Sauer C, Perkins TT (2015) Ultrastable measurement platform: sub-nm drift over hours in 3D at room temperature. Opt Express 23:16554–16564
- 23. Capitanio M, Cicchi R, Pavone FS (2005) Position control and optical manipulation for nanotechnology applications. Eur Phys J B 46:1–8
- 24. Janshoff A, Neitzert M, Oberdorfer Y, Fuchs H (2000) Force spectroscopy of molecular systems single molecule spectroscopy of polymers and biomolecules. Angew Chem Int Ed Engl 39:3213–3237
- Churnside AB, King GM, Carter AR, Perkins TT (2008) Improved performance of an ultrastable measurement platform using a fieldprogrammable gate array for real-time deterministic control. Proc SPIE 7042:704205